Molecular Monolayers and Interfacial Electron Transfer of *Pseudomonas aeruginosa* Azurin on Au(111)

Qijin Chi,[†] Jingdong Zhang,[†] Jens U. Nielsen,[†] Esben P. Friis,[†] Ib Chorkendorff,[‡] Gerard W. Canters,[§] Jens E. T. Andersen,[†] and Jens Ulstrup*[,†]

Contribution from the Department of Chemistry, Building 207, and Department of Physics, Building 307, Technical University of Denmark, DK-2800 Lyngby, Denmark, and Gorlaeus Laboratory, Department of Chemistry, Leiden University, 2333 CC, The Netherlands

Received September 2, 1999

Abstract: We provide a comprehensive approach to the formation and characterization of molecular monolayers of the blue copper protein *Pseudomonas aeruginosa* azurin on Au(111) in aqueous ammonium acetate solution. Main issues are adsorption patterns, reductive desorption, properties of the double layer, and long-range electrochemical electron transfer between the electrode and the copper center. Voltammetry, electrochemical impedance spectroscopy (EIS), in situ scanning tunneling microscopy (STM), and X-ray photoelectron spectroscopy (XPS) have been employed to disclose features of these issues. Zn-substituted azurin, cystine, and 1-butanethiol are investigated for comparison. Cyclic voltammetric and capacitance measurements show *qualitatively* that azurin is adsorbed at submicromolar concentrations over a broad potential range. The characteristics of reductive desorption suggest that azurin is adsorbed via its disulfide group to form a monolayer. The adsorption of this protein on Au(111) via a gold−sulfur binding mode is further supported by XPS measurements. In situ STM images with molecular resolution have been recorded and show a dense monolayer organization of adsorbed azurin molecules. Direct electron transfer (ET) between the copper atom of adsorbed azurin and the electrode has been revealed by differential pulse voltammetry. The rate constant is estimated from electrochemical impedance spectroscopy and shows that ET is compatible with a long-range ET mode such as that anticipated by theoretical frames. The results constitute the first case of an electrochemically functional redox protein monolayer at single-crystal metal electrodes.

Introduction

Natural protein function is ubiquitously associated with interfaces between aqueous solutions and solids or membranes. This has prompted extensive interdisciplinary investigations of fabrication, characterization, and theoretical notions of functional mono- and multilayers of proteins at interfaces.[1] Such explorations have given us many perspectives on both the fundamental properties of biological processes and the technological design of biosensing devices. The former refers, for example, to control of adsorbed protein function,[2] electron exchange at interfaces,[3] and functional relationships to protein conformational changes.[4] Technological perspectives are associated, for example, with biosensors, photoinduced interfacial electronics, analytical chemical devices, and microbial corrosion.[5,6] Arrays of proteins with a well-defined organization on substrates have been proved to be a key step in interfacial protein engineering. To this end, Langmuir−Blodgett (LB) techniques have been extensively used and are efficient for many proteins.[1a,b] Another approach involves immobilization of proteins on self-assembled monolayers (SAMs) of small organic molecules.[7]

A variety of techniques have been applied to reveal the structure and function of immobilized proteins at interfaces.[1a] Among these, electrochemistry and in situ scanning tunneling microscopy (STM) could become central, particularly in the context of redox metalloproteins. STM is a powerful means to map surface structure and electronic properties of immobilized proteins at the molecular level. However, it is essential that STM

* To whom correspondence should be addressed. Phone: +45 45252359. Fax: +45 45883136. E-mail: ju@kemi.dtu.dk.

[†] Department of Chemistry, Technical University of Denmark.

[‡] Department of Physics, Technical University of Denmark.

[§] Department of Chemistry, Leiden University.

(1) (a) Lösche, M. *Curr. Opin. Solid State Mater. Sci.* **1997**, *2*, 546−556. (b) Sackmann, E. *Science* **1996**, *271*, 43−48. (c) Nagayama, K. In *Protein Array: an alternative biomolecular system*; Nagayama, K., Ed.; Advances in Biophysics 34; Japan Scientific Press: Tokyo, 1997; pp 3−23.

(2) (a) *Surface and Interfacial Aspects of Biomedical Polymers, Vol. 2, Protein Adsorption*; Andrade, J. D., Ed.; Plenum: New York, 1985. (b) *Proteins at interfaces II*; Brash, J. L., Horbertt, Eds.; ACS Symposium Series 602; American Chemical Society: Washington, DC, 1995.

(3) (a) Armstrong, F. A. *Struct. Bond* **1990**, *72*, 137−221. (b) Hill, H. A. O.; Hunt, N. I. *Methods Emzymol.* **1993**, *227*, 501−522. (c) Armstrong, F. A.; Heering, H. A.; Hurst, J. *Chem. Soc. Rev.* **1997**, *26*, 169−179.

(4) (a) Norde, W. *Adv. Colloid Interface Sci.* **1986**, *25*, 267−340. (b) Tobias, D. J.; Mar, W.; Blasie, J. K.; Klein, M. L. *Biophys. J.* **1996**, *71*, 2933−2941.

(5) (a)*Biosensors: Fundamentals and Applications*; Turner, A. P. F., Karube, I., Wilson, G., Eds.; Oxford University Press: London, 1989. (b) Willner, I.; Katz, E.; Willner, B.; Blonder, R.; Heleg-Shabtai, V.; Buckman, A. F. *Biosens. Bioelectron.* **1997**, *12*, 337−356 and references therein.

(6) Telegdi, J.; Keresztes, Z.; Palinkas, G.; Kalaman, E.; Sand, W. *Appl. Phys. A* **1998**, *66*, S639−S642.

(7) See, for example: (a) Tarlov, M. J.; Bowden, E. F. *J. Am. Chem. Soc.* **1991**, *113*, 1847−1849. (b) Collinson, M.; Bowden, E. F.; Tarlov, M. J. *Langmuir* **1992**, *8*, 1247−1250. (c) Song, S.; Clark, R. A.; Bowden, E. F.; Tarlov, M. J. *J. Phys. Chem.* **1993**, *97*, 6564−6572. (d) Feng, Z.-Q.; Imabayashi, S.; Kakiuchi, T.; Niki, K. *J. Electroanal. Chem.* **1995**, *394*, 149−154. (e) Jiang, M.; Nolting, B.; Stayton, P. S.; Sligar, S. G. *Langmuir* **1996**, *12*, 1278−1283. (f) Madoz, J.; Kutznetzov, B. A.; Medrano, F. J.; Garcia, J. L.; Fernandez, V. M. *J. Am. Chem. Soc.* **1997**, *119*, 1043−1051. (g) Wood, L. L.; Cheng, S.-S.; Edmiston, P. L.; Saavedra, S. S. *J. Am. Chem. Soc.* **1997**, *119*, 571−576. (h) Dong, S.; Li, J. *Bioelectrochem. Bioenerg.* **1997**, *42*, 7−13. (i) Burgess, J. D.; Rhoten, M. C.; Hawkridge, F. M. *J. Am. Chem. Soc.* **1998**, *120*, 4488−4491. (j) Burgess, J. D.; Rhoten, M. C.; Hawkridge, F. M. *Langmuir* **1998**, *14*, 2467−2475.

10.1021/ja993174t CCC: $19.00
Published on Web 04/12/2000

mapping is implemented in the in situ mode, directly in the natural aqueous medium for protein function. Full and separate substrate and tip potentiostatic control is, moreover, crucial. Meanwhile, the introduction of single-crystal electrodes, ultrapure conditions, and interfacial spectroscopic techniques known from surface physics has played a great role in the development of electrochemistry into a highly sophisticated interdisciplinary surface science. Electrochemistry of biomacromolecules, and the approaching option of combining bioelectrochemistry with molecular approaches such as in situ STM, now warrant a broader interface with these achievements of physical electrochemistry.

The main focus of this report is on surface molecular architecture and interfacial electron transfer (ET) of redox metalloproteins at single-crystal metal substrates. Major issues are the formation, surface structure, electronic properties, and interfacial ET dynamics of monolayers, specifically of the blue copper protein *Pseudomonas aeruginosa* azurin. Bulk structural, electronic, and kinetic properties of this class of proteins have been well characterized.[8−12] Figure 1A shows the three-dimensional structure of *P. aeruginosa* azurin.[9] In particular, patterns for intramolecular ET between the copper atom and either the radical anion of a surface disulfide group (Cys3Cys26),[8b,9] nearly opposite to the strongly asymmetrically located copper atom, or covalently attached electron exchanging groups,[10] have been mapped. The disulfide group is, moreover, a suitable linker group to soft metal substrates, as disclosed by a number of observations at the molecular level described below. A theoretical framework for STM electronic properties[13a,b] and preliminary electrochemical investigations[13c] of adsorbed azurin have been addressed recently. In the present work, we provide a comprehensive and systematic investigation of self-assembled monolayers of *P. aeruginosa* azurin on Au(111), based on a *combination* of electrochemistry, in situ STM, and XPS techniques.

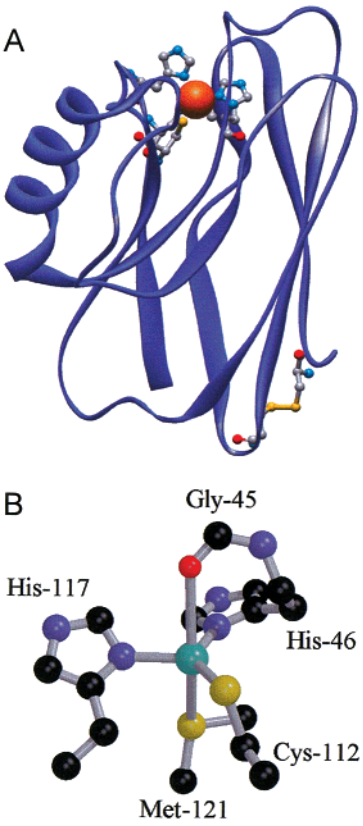

Figure 1. (A) Three-dimensional structure of *P. aeruginosa* azurin. Coordinates from ref 12a and Brookhaven Protein Data Bank and Molscript representation according to ref 12b. (B) The coordinating ligands of the copper atom in the azurin molecule.

Experimental Section

Chemicals. *P. aeruginosa* azurin (i.e., Cu-azurin) from Sigma was purified as previously described.[14] Zn-azurin was prepared according to reported procedures.[15] Cystine from Fluka and 1-butanethiol from Merck were used without further purification. All other reagents used in preparing solutions were of ultrapure grade. NH_4Ac solution (50 mM, pH 4.6−7.0) was prepared from 5 M stock solution (Fluka, ultrapure), and the solution pH was adjusted with $HClO_4$ (70%, Fluka, ultrapure grade). $NaClO_4$ solution (50 mM, pH 4.6) was prepared by mixing $HClO_4$ with sodium hydroxide (30%, Merck, suprapure). NaOH solution (0.1 M, pH 13) was prepared by diluting 30% stock solution (Merck, suprapure). Millipore water (Milli-Q Housing, 18.2 MΩ) was used throughout.

Preparation of Au(111) Substrates. Gold single-crystal beads were made by melting the ends of Au wire (0.8 or 1.0 mm in diameter) according to the method of Clavilier et al.[16a] and Hamelin.[16b] The Au(111) facets formed on the single-crystal bead were used for STM measurements. Mechanically exposed Au(111) surfaces were used for electrochemical and XPS measurements. The quality of the electrodes was checked by recording the cyclic voltammograms (CVs) of 0.1 M $HClO_4$, which was found to be consistent with reported CVs.[16b]

Preparation of Samples. The Au(111) electrode was annealed in a hydrogen flame and quenched in ultrapure water saturated with dihydrogen. The electrode was then immediately immersed in azurin-containing solutions for several hours, followed by careful rinsing with pure water. In an alternative procedure azurin was added directly to the solution. Similar procedures were used in other sample preparations for reference molecules.

Electrochemical Measurements. The hang meniscus method[16] was used for electrochemical measurements. In this method the particular metal plane of the single-crystal electrode is brought into contact with the electrolyte solution by forming a meniscus. Details and operation of the method have been described recently.[16c] Cyclic voltammetry, differential pulse voltammetry (DPV), linear scan voltammetry (LSV), capacitance, and ac impedance measurements were undertaken using

(8) (a) Sykes, A. G. *Adv. Inorg. Chem.* **1991**, *36*, 377−408. (b) Farver, O. In *Protein Electron Transfer*; Bendall, D., Ed.; BIOS Publishers: Oxford, 1996; pp 161−188.

(9) Farver, O.; Pecht, I. *J. Am. Chem. Soc.* **1992**, *114*, 5764−5767.

(10) (a) Gray, H. B.; Winkler, J. R. *Annu. Rev. Biochem.* **1996**, *65*, 537−561. (b) Winkler, J. R.; Gray, H. B. *J. Biol. Inorg. Chem.* **1997**, *2*, 399−404 and references therein.

(11) (a) Karlsson, B. G. Protein Engineering on Azurin. Expression, Mutagenesis and Characterization of Copper Site Mutants. Dissertation, Chalmers University of Gothenburg and Goteborg University, 1993. (b) Canters, G. W.; van Pouderoyen, M. *Biosens. Bioelectron.* **1994**, *9*, 637−645. (c) Kroes, S. J.; Salgado, J.; Parigi, G.; Luchinat, C.; Canters, G. W. *J. Biol. Inorg. Chem.* **1996**, *1*, 551−559 and references therein.

(12) (a) Nar, H.; Messerschmidt, A.; Huber, R. *J. Mol. Biol.* **1991**, *221*, 765−772. (b) Kraulis, P. *J. Appl. Crystallogr.* **1991**, *24*, 946−950.

(13) (a) Friis, E. P.; Kharkats, Yu. I.; Kuznetsov, A. M.; Ulstrup, J. *J. Phys. Chem. A* **1998**, *102*, 7851−7859. (b) Friis, E. P.; Andersen, J. E. T.; Kharkats, Yu. I.; Kuznetsov, A. M.; Nichols, R. J.; Zhang, J. D.; Ulstrup, J. *Proc. Natl. Acad. Sci. U.S.A.* **1999**, *96*, 1379−1384. (c) Chi, Q.; Zhang, J. D.; Friis, E. P.; Andersen, J. E. T.; Ulstrup, J. *Electrochem. Commun.* **1999**, *1*, 91−96.

(14) Friis, E. P.; Andersen, J. E. T.; Madsen, L. L.; Møller, P.; Bonander, N.; Ulstrup, J. *Electrochim. Acta* **1997**, *42*, 2889−2897; *Electrochim. Acta* **1998**, *43*, 1113−1122 (erratum).

(15) (a) Van de Kamp, M.; Hali, F. C.; Rosato, N., Finazzi-Agro, A.; Canters, G. W. *Biochim. Biophys. Acta* **1990**, *1019*, 283−292. (b) Nar, H.; Huber, R.; Messerschmidt, A.; Filipou, A. C.; Barth, M.; Jaquinod, M.; Van de Kamp, M.; Canters, G. W. *Eur. J. Biochem.* **1992**, *205*, 1123−1129.

(16) (a) Clavalier, J.; Faure, R.; Guinet, G.; Durand, R. *J. Electroanal. Chem.* **1980**, 107, 205−209. (b) Hamelin, A. *J. Electroanal. Chem.* **1996**, *411*, 1−12. (c) Aramata, A. In *Modern Aspects of Electrochemistry*; Bockris, J. O'M., White, R. E., Conway, B. E., Eds.; Plenum Press: New York, 1997; No. 31, p 185.

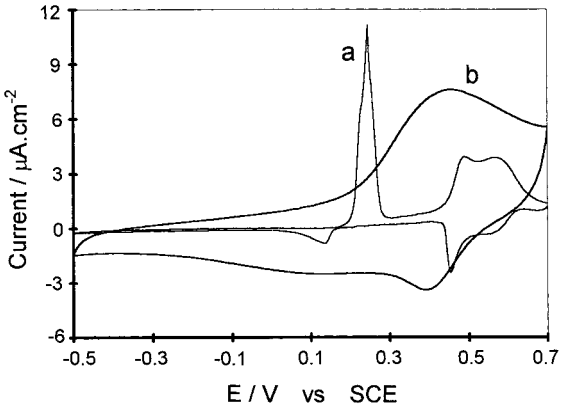

Figure 2. Cyclic voltammograms of Au(111) in 50 mM NH_4Ac (pH 4.6): (a) bare and (b) azurin-adsorbed electrodes. Scan rate, 50 mV s^{-1}.

an Autolab system (Eco Chemie, Netherlands) controlled by general-purpose electrochemical system software. Parameters used in DPV and capacitance measurements were described previously.[13c] Electrochemical impedance spectra of adsorbed azurin were acquired at fixed potential (typically 0.1 V vs SCE) with a modulation amplitude of 5 mV and analyzed using a complex nonlinear least-squares (CNLS) computer program. A bright platinum wire was the counter electrode, while a reversible hydrogen electrode (RHE) freshly exposed to the same supporting electrolyte and bubbled with pure dihydrogen prior to use was the reference electrode. The RHE was always checked against a saturated calomel electrode (SCE) after each measurement. All electrode potentials are referred to the SCE. Purified argon (Chrompack, 5 N) was applied to deoxygenate all solutions. An argon stream over the solution was always maintained during the measurements.

In Situ STM Imaging. A commercial Rasterscope 3000-EC instrument (DME, Denmark) equipped with a bipotentiostat for independent potential control of both substrate and tip was used. Electrochemical control was conducted in a homemade cell with a special design that enables compatibility with the STM instrument by using a three-electrode system. All STM images were acquired in the constant-current mode and are reported as raw data.

XPS Analyses. The XPS spectra were obtained with a Perkin-Elmer surface analysis system (Physical Electronic Industries Inc., USA) equipped with a magnesium source and a multichannel detector. The base pressure in the chamber during the data acquisition was kept below 8×10^{-10} Torr. Pass energy of either 25.0 or 50.0 eV was used. All spectra are referenced to Au($4f_{7/2}$) at 84.00 eV.

All measurements were conducted at room temperature. Glassware was cleaned as described previously.[13c]

Results and Discussion

Interfacial Capacitance and Cyclic Voltammetry of Au(111) in NH_4Ac. The aqueous electrolyte used in the present work was mostly 50 mM ammonium acetate (pH 4.6), which is a commonly used medium for azurin research. The isoelectric point of azurin occurs at pH = 4.6. The dynamic electrochemical features of Au(111) in this medium were first examined, as no standard CV and capacitance data are available, unlike for Au(111) in perchlorate or other solutions.[16b] Cyclic voltammograms with various potential windows were recorded. The most suitable potential window for subsequent observation of azurin adsorption was found in the range from −0.5 to 0.7 V vs SCE. From well-defined CVs for bare Au(111) in this potential range, the most striking feature is a *sharp* anodic peak matched by a small cathodic peak (Figure 2, curve a). The peak position and current depend on solution pH. Anodic and cathodic peaks appear at about 0.25 and 0.15 V at pH 4.6, respectively. The peaks are shifted negatively and increased with increasing solution pH. The potential-dependent capacitance curves recorded in the same potential range show that the maximum capacitance hump appears at positions compatible with the sharp anodic peak in the CV. The characteristic peaks are most likely associated with adsorption and desorption of acetate. This is supported by additional experiments. In 50 mM $NaClO_4$ solution (pH 4.6), no characteristic voltammetric peaks are observed. The addition of NH_4Ac, however, invoked such responses. The response increased with increasing NH_4Ac concentration toward a limit around 10 mM. Similar patterns were observed in the capacitance measurements. Other evidence is available from in situ STM in 50 mM NH_4Ac (pH 4.6) at various working potentials. Only the clean Au(111) surface was observed below 0.1 V, while an adlayer appeared at substrate potentials positive of 0.2 V, where the characteristic anodic peak commences.

The adsorbate could be either Ac^- or HAc. Corrigan et al. concluded that adsorption of acetic acid occurs on polycrystalline Au (poly-Au) close to the potentials where gold oxide formation commences, but no adsorption of *acetate anions* could be detected.[17] We believe, however, that adsorption from NH_4Ac on Au(111) is more likely to be dominated by the *acetate anion*, as the characteristic anodic peak in 50 mM NH_4Ac (pH 6.8) is larger and appears at more negative potential than that in 50 mM HAc (pH 3.0). The apparent disparity is possibly due to the structural difference between poly-Au and Au(111) surfaces, since no characteristic peaks could be observed at a poly-Au electrode in acetate-containing solution from our reference experiments.

Formation of Adlayers. As noted in the Experimental Section, two ways to obtain adlayers of azurin and reference molecules on Au(111) were used. One involves addition of azurin directly to the blank medium under potentiostatic control, and the other involves the preadsorption by immersing Au(111) in azurin-containing solution. The two methods give similar results. Figure 2 shows CVs of bare (a) and azurin-adsorbed (b) electrodes in azurin-free solution. The presence of the azurin adlayer totally inhibits the characteristic anodic peak at 0.25 V. Considerable changes in the double-layer region are also observed and are discussed below.

By using the former method (i.e., gradual addition of azurin directly to the blank medium), observation of dynamic formation of the adlayer may be accomplished by recording systematic changes in the CVs and capacitance curves. Addition of submicromolar concentrations of azurin invokes marked changes in voltammetric and capacitance responses. The most conspicuous effects appear as *gradual* attenuation of the characteristic anodic peak or capacitance hump around 0.25 V with increasing concentration of azurin, approaching saturation at about 0.2 μM. Similar patterns were observed for cystine and butanethiol where, however, much larger amounts (about 20- and 50-fold for cystine and butanethiol, respectively) are required to invoke a similar effect. The large difference in concentration accords qualitatively with the widely different molecular dimensions. Similar measurements were performed with Zn-azurin, with no detectable difference from Cu-azurin, indicating that a similar adlayer of Zn-azurin is formed.

These observations indicate *qualitatively* that azurin is strongly adsorbed at submicromolar concentrations, in a broad potential range. Adsorption seems to proceed through gradual replacement of acetate on the Au(111) surface. The qualitatively similar patterns of azurin and small organic thiolates imply that the adsorption of azurin occurs via the disulfide group to form

(17) Corrigan, D. S.; Krauskopf, E. K.; Rice, L. M.; Wieckowski, A.; Weaver, M. J. *J. Phys. Chem.* **1988**, *92*, 1596−1601.

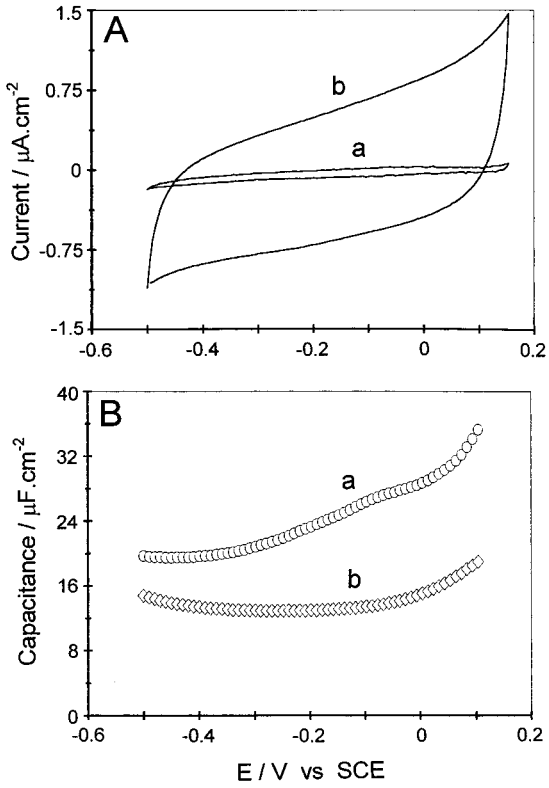

Figure 3. (A) Cyclic voltammograms and (B) potential-dependent capacitance curves of Au(111) in 50 mM NH_4Ac (pH 4.6): (a) bare and (b) azurin-adsorbed electrodes. Scan rate, 50 mV s^{-1} for CVs.

monolayers. More convincing evidence for this comes from studies of reductive desorption, XPS, and in situ STM, which are addressed below.

Double-Layer Properties. We have examined the properties of the electrochemical double layer before and after deposition of the target molecules on Au(111). Apparent inflation in charging currents of the CVs is observed in the presence of either azurin or cystine in solution. The inflation *increases* with increasing concentration toward saturation at about 0.2 μM for azurin and 5 μM for cystine. Charging currents in the CVs decrease in the presence of butanethiol. Potential-dependent capacitance curves show, however, that the interfacial capacitance decreases in the presence of all the three target molecules. The observations for butanethiol are similar to previous reports for alkane SAMs.[18,19] Figure 3 shows typical CVs (A) and capacitance curves (B) in the double-layer region for bare (curves a) and azurin-adsorbed (curves b) electrodes in azurin-free solution. The presence of an azurin adlayer (saturated) results in a 7−10-fold increase in the charging current of CV (Figure 3A) but a notable decrease (ca 40%) in capacitance (Figure 3B). This means that the increase in charging current is not caused by the capacitance change and the discrepancy between CV and capacitance measurements cannot be explained by the classical Helmholtz model.

The double-layer capacitance for alkanethiol SAMs on Au electrodes has usually been estimated from the charging current of CV.[18,19] The capacitance depends strongly on the type of terminating groups. SAMs terminated with hydrophobic groups (typically denoted as HSC_nCH_3 SAMs) cause a dramatic decrease in capacitance due to a low dielectric constant between the electrode and the electrolyte. A linear relationship between the reciprocal of the interfacial capacitance and the chain length is also established when the alkane chain has 10 or more methylene units.[18a] For HSC_nCOOH SAMs (i.e., terminated by hydrophilic groups), the situation is less straightforward. Theoretical models have been developed by taking the monolayer capacitance (C_m), solvated capacitance (C_s), and diffuse layer capacitance (C_d) into account,[18b−e] but they can only *in part* explain the experimental observations. A difference between HSC_nCOOH and azurin monolayers is that the former is hydrophilic only at the carboxyl group moiety while the latter is largely hydrophilic through the whole monolayer and contains both hydrophilic and hydrophobic surface groups. The latter is also in both positive and negative charge states. The effects of solvation and diffusion could thus be more important in determining the double-layer properties for the azurin-adsorbed electrode.

Reductive Desorption. Reductive desorption is one of the most important properties of monolayers adsorbed via the gold−sulfur bond mode. The use of electrochemical methods to disclose this feature was initiated by Porter et al.[20] Cyclic and linear scan voltammetries (LSV) are usually combined with KOH electrolyte (pH > 11) for the SAMs of small organic thiolates to avoid protonation of the liberated thiolate. Cathodic peaks are indications of the reduction reaction of the gold−sulfur bond breaking, and the surface coverage of adlayers can be estimated from the charge generated.

The desorption behavior of azurin on Au(111) was investigated in various media. No reductive desorption peak in NH_4-Ac (pH 4.6 or 6.8) could be detected, due to overlap with hydrogen evolution. LSV of the azurin-adsorbed electrodes in azurin-free NaOH solution (pH 13), however, gives a main desorption peak at -900 ± 30 mV and an additional small peak around −1.0 V in the first scan, which disappear in the second and following scans as expected, and implies that desorption might be a multistep process. Integration of the peak in the first scan shows that the charge is close to that of a closed-packed monolayer of azurin. The reductive desorption behavior of azurin can be better disclosed by using more sensitive DPV measurements.[13c] The surface coverage estimated from the Faradaic charge of the DPV peak is $(7.0 \pm 0.5) \times 10^{-12}$ mol·cm^{-2}, i.e., close to a monolayer. The reliability of estimating the charge from DPV measurements, references to data for cystine and butanethiol, and discussion of the desorption mechanisms are given in refs 13c and 21.

Desorption of azurin occurring at potentials negative of cystine desorption (by at least 200 mV) could be due to the large difference in molecular dimensions between cystine and azurin. Such size effects are well-known for alkanethiol SAMs.[20] The desorption peak of the latter is usually located in the range from −0.65 to −1.35 V (vs SCE) and depends on the length of the alkane chain: longer chains give peaks at more negative potentials. The desorption characteristics thus substantiate that azurin is adsorbed on Au(111) in a monolayer via the disulfide group.

(18) (a) Porter, M. D.; Bright, T. B.; Allara, D. L.; Chidsey, C. E. D. *J. Am. Chem. Soc.* **1987**, *109*, 3559−3568. (b) Smith, C. P.; White, H. S. *Anal. Chem.* **1992**, *64*, 2398−2405. (c) Smith, C. P.; White, H. S. *Langmuir* **1993**, *9*, 1−8. (d) Andreu, R.; Fawcett, W. R. *J. Phys. Chem.* **1994**, *98*, 12753−12758. (e) Fawcett, W. R.; Fedurco, M.; Kovacova, Z. *Langmuir* **1994**, *10*, 2403−2408.

(19) Finklea, H. O. In *Electroanalytical Chemistry*; Bard, A. J., Ed.; Marcel Dekker: New York, 1996; Vol. 19, pp 109−335 and references therein.

(20) (a) Widrig, C. A.; Chung, C.; Porter, M. D. *J. Electroanal. Chem.* **1991**, *310*, 335−359 and references therein. (b) Walczak, M. M.; Popenoe, D. D.; Deinhammer, R. S.; Lamp, B. D.; Chung, C.; Porter, M. D. *Langmuir* **1991**, *7*, 2687−2693. (c) Zhong, C. J.; Porter, M. D. *J. Am. Chem. Soc.* **1994**, *116*, 11616−11617. (d) Walczak, M. M.; Alves, C. A., Lamp, B. D.; Porter, M. D. *J. Electroanal. Chem.* **1995**, *396*, 103−114. (e) Zhong, C. J.; Brush, R. C.; Anderegg, J.; Porter, M. D. *Langmuir* **1999**, *15*, 518−525.

XPS Analysis. XPS has been established as an additional powerful tool to characterize the structure of alkanethiol SAMs.[20,22] We have compared XPS spectra of bare Au(111), azurin, cystine, and butanethiol adsorbed on Au(111). Survey spectra with the binding energy range of 0−1000 eV were first recorded and confirm the presence of the appropriate chemical elements in each sample (data not shown). For azurin-adsorbed Au(111), carbon, nitrogen, and copper signals together with weak signals from sulfur were detected. The presence of an azurin adlayer results in a marked lowering of the Au(4f) intensity in comparison with that of bare Au(111), while the effects caused by cystine and butanethiol films are much smaller. The observations accord *qualitatively* with the thickness of self-assembled monolayers arising from the size difference of the molecules (the thickness of an azurin monolayer is more than 30 Å, if tilting of adsorbed protein molecules can be disregarded). Subsequent characterization is then focused on the characteristic spectral regions. Representative results for the N(1s) region are shown in Figure 4A. The azurin on Au(111) gives a large well-defined peak around 401 eV (Figure 4A, curve a), whereas a considerably smaller response and no detectable signal are found for cystine (Figure 4A, curve b) and butanethiol (Figure 4A, curve c), respectively. These results are consistent with the composition of and amount of nitrogen in the samples. Figure 4B shows high-resolution XPS spectra for the S(2p) region. Almost the same pattern is observed for cystine (Figure 4B, curve b) and butanethiol (Figure 4B, curve c) Au(111) samples. The S(2p) spectra exhibit a doublet at 163.3 ($2p_{1/2}$) and 162.2 eV ($2p_{3/2}$), which are typically characteristic of interaction of the sulfur headgroup with the gold surface[23] and agree well with previous reports for alkanethiol SAMs on gold.[20c,d]

Three peaks from S(2p) can, in fact, be distinguished (Figure 4B, curve a) for the azurin-adsorbed Au(111) samples. Two are qualitatively similar to those for cystine and butanethiol and are caused by the sulfur−gold bond. An additional peak appears at 164.1 eV. The assignment of this peak is not completely clear at present, but it could be caused by the two additional S atoms in methionine and cysteine (Figure 1B). Together with two histidines and a glutamate, these groups are coordinated to the copper atom.[24] Qualitative angle-dependent measurements show, further, that the intensity ratio of the peak at 164.1 eV to the peak at 162.2 eV is enhanced by lowering the takeoff angle. This observation confirms that the two peaks result from S atoms with different locations, and the peak at 164.1 eV should originate from S atoms located in the upper part of the azurin film on Au(111). This accords with the fact that methionine and cysteine S atoms coordinating with copper are located nearly opposite to the surface disulfide group (Cys3Cys26) (Figure 1A) linking azurin to the gold surface. XPS spectra thus provide additional evidence that azurin is adsorbed via the sulfur binding to gold.

In Situ STM Observations. STM imaging of proteins in ambient air environment has been known for over a decade,[25] but the feasibility of redox protein imaging in the in situ STM mode is quite recent, and available reports are still few in number.[26] Difficulties are associated particularly with the preparation of stable and ordered monolayers of proteins in addition to the operation of the in situ STM itself. Monolayers of azurin on Au(111) have come to be robust enough for STM imaging to disclose surface structures of individual immobilized protein molecules. A series of high-resolution STM images with various scan areas in 50 mM NH_4Ac (pH 4.6) under potentiostatic control were obtained. Two representative images in raw data form are shown in Figure 5. STM images with a large scan area show a close-packed monolayer structure for azurin adsorbed on Au(111) to saturation. Individual molecules are clearly discerned in the STM images (Figure 5). Average lateral

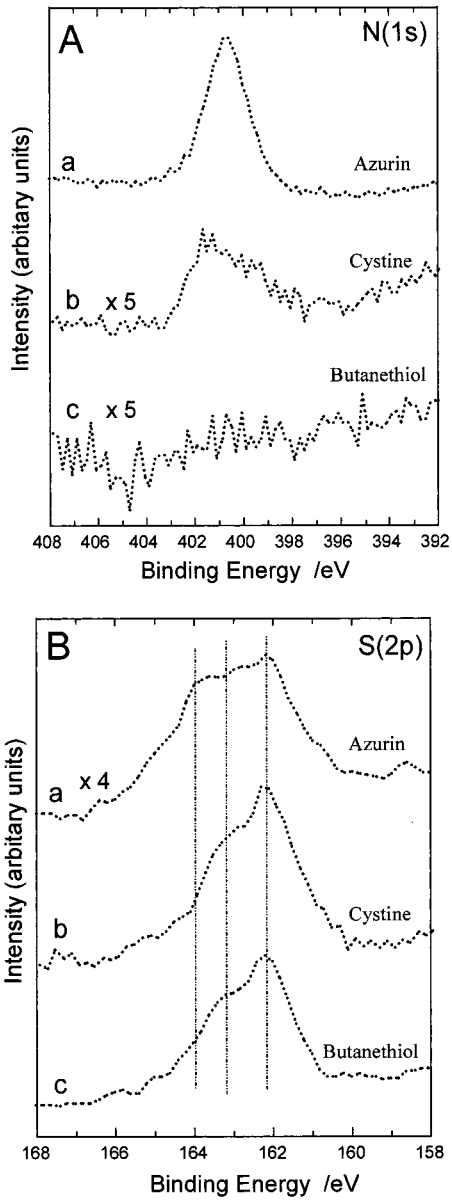

Figure 4. XPS spectra in the regions of N_{1s} (A) and S_{2p} (B) for Au(111) substrates adsorbed with various target molecules: (a) azurin, (b) cystine, and (c) butanethiol. Pass energy, 25 eV.

(21) Zhang, J.; Chi, Q.; Ulstrup, J.; et al. manuscript in preparation.

(22) (a) Bain, C. D.; Troughton, E. B.; Tao, Y.-T.; Evall, J.; Whitesides, G. M.; Nuzzo, R. G. *J. Am. Chem. Soc.* **1989**, *111*, 321−335. (b) Bain, C. D.; Evall, J.; Whitesides, G. M. *J. Am. Chem. Soc.* **1989**, *111*, 7155−7164.

(23) Lindberg, B. J.; Hamrin, G.; Johanson, G.; Gelius, U.; Fahlman, A.; Nording, C.; Siegbahn, K. *Phys. Scr.* **1970**, *1*, 286−298.

(24) For the details of structure of azurin molecule, see for example ref 12a and the following: Adman, E. T.; Jensen, L. H. *Isr. J. Chem.* **1981**, *21*, 8−12.

(25) (a) Chen, C. J. *Introduction to Scanning Tunneling Microscopy*; Oxford University Press: New York, 1993. (b) Magonov, S. N.; Whangbo, M. H. *Surface Analysis with STM and AFM*; Verlag Chemie: Weinheim, 1996. (c) *SPM and SFM in Biology*; Marti, O., Amrein, M., Eds.; Academic Press: San Diego, CA, 1993.

(26) See for example: (a) Andersen, J. E. T.; Møller, P.; Pedersen, M. V.; Ulstrup, J. *Surf. Sci.* **1995**, 325−332. (b) Zhang, J.; Chi, Q.; Dong, S.; Wang, E. *Bioelectrochem. Bioenerg.* **1996**, *39*, 267−274. (c) Andersen, J. E. T.; Olesen, K. G.; Danilov, A. I.; Foverskov, Møller, P.; Ulstrup, J. *Bioelectrochem. Bioenerg.* **1997**, *44*, 57−63.

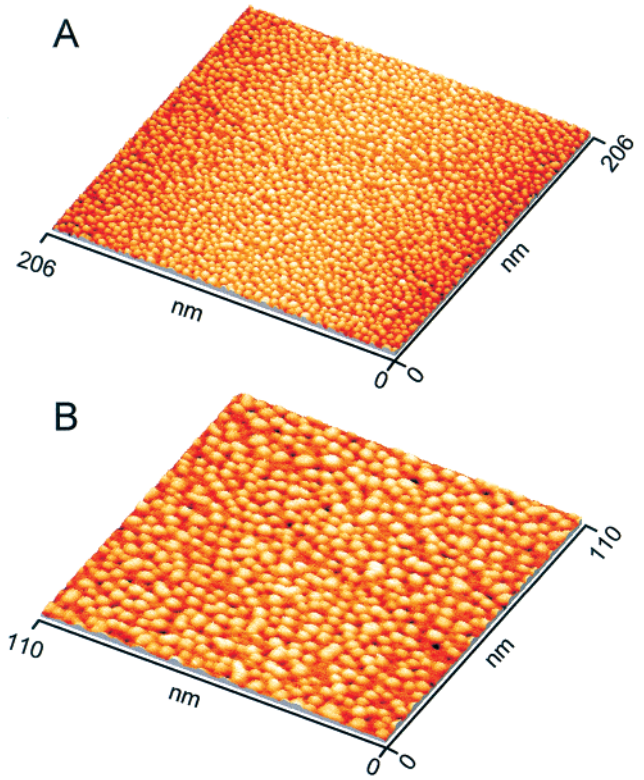

Figure 5. In situ STM images (raw data) of azurin-adsorbed Au(111) in 50 mM NH_4Ac (pH 4.6) obtained in the constant-current mode. Scan area: (A) 206 nm × 206 nm, (B) 110 nm × 110 nm. Bias voltage, 0.2 V; tunnel current, 1.0 nA; and working potential, −0.1 V vs SCE.

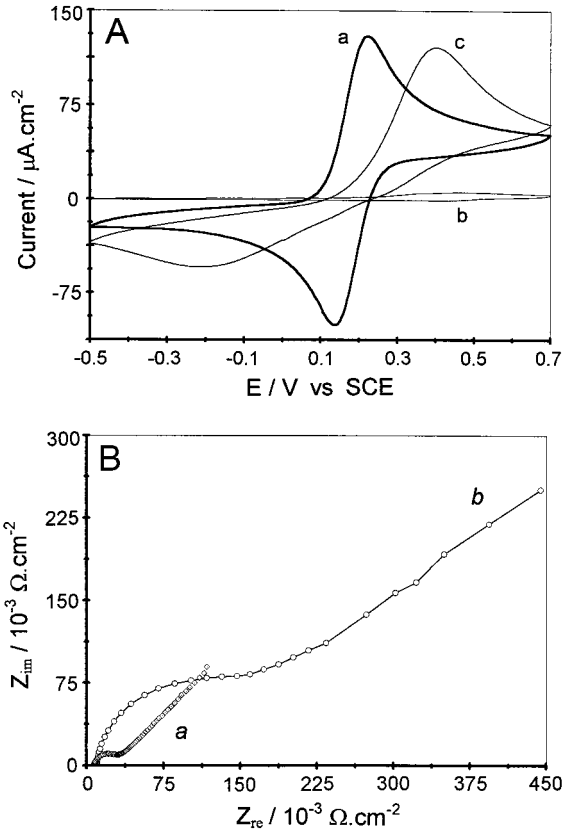

Figure 6. (A) Cyclic voltammograms of (a) bare Au(111) in 50 mM NH_4Ac (pH 4.6) containing 2 mM $K_4[Fe(CN)_6]$, (b) azurin-adsorbed Au(111) in 50 mM NH_4Ac (pH 4.6), and (c) 50 mM NH_4Ac (pH 4.6) containing 2 mM $K_4[Fe(CN)_6]$. Scan rate, 50 mV s^{-1}. (B) Electrochemical impedance spectra of (a) bare and (b) azurin-adsorbed Au(111) in 50 mM NH_4Ac (pH 4.6) containing 2 mM $K_4[Fe(CN)_6]$. Potentials applied were set at formal potentials of the redox system (i.e., 0.19 V vs SCE in the present medium). The frequency is from 0.01 Hz to 10 kHz.

molecular dimensions are 3.7 ± 0.4 nm, which is close to those obtained from X-ray crystallography. The estimated height is, however, only 1.2 ± 0.2 nm, which is significantly smaller than the physical height of azurin molecules. Such a discrepancy has also been found in STM imaging of other proteins. The precise origin is presently elusive but is usually referred to the work function difference between substrate and adsorbate.[26b]

The surface coverage of azurin adsorbed on Au(111) can be *empirically* controlled by adjusting temperature, adsorption time, and azurin concentration. Samples with various surface coverages of ca. 30%−70% of a close-packed monolayer were prepared and investigated by in situ STM. No observable differences in STM image resolution and individual molecular dimensions were found compared to those of the close-packed monolayer. This implies that lateral interactions between adsorbed protein molecules may be weak. The stability of the azurin monolayer was also examined. A freshly prepared sample with a close-packed monolayer of azurin was imaged immediately. It was then stored in azurin-free solution at 4 °C and reimaged once a week under the same experimental conditions. STM images similar to those shown in Figure 5 were consistently obtained. No apparent changes in population and dimensions for adsorbed azurin molecules were observed over *three* weeks. After three weeks, the population slightly decreased and the dimensions became larger. The latter could be due to the partial unfolding of adsorbed protein molecules. These observations thus demonstrate that monolayers of azurin on Au(111) are quite robust.

Redox Probe. Structural properties of the azurin monolayer, such as density and defects, can be further disclosed by using small redox couples as probes. This method has previously been applied to alkanethiol SAMs, from which interesting information can be extracted.[27] $K_4[Fe(CN)_6]$ in 50 mM NH_4Ac (pH 4.6) was used in both cyclic voltammetry and electrochemical impedance spectroscopy (EIS) in the present study. A symmetric CV with a modest peak separation of 75 ± 5 mV is observed at bare Au(111) (Figure 6A, curve a), indicating that the redox reaction is quasi-reversible. The linear dependence of the peak current on the square root of the scan rate further indicates that the reaction is diffusion-controlled. The presence of an azurin monolayer results in a strongly asymmetric CV with markedly smaller cathodic currents and a large peak separation of 600 ± 50 mV (Figure 6A, curve c). Both anodic and cathodic peaks at the azurin-adsorbed electrode follow the square root dependence of the sweep rate, indicating that the reaction is still a diffusion-controlled process. Apparent rate constants estimated from the peak separation show that the reaction is attenuated by at least 2 orders of magnitude by the azurin monolayer. This is further confirmed by the EIS measurements shown in Figure 6B.

The following mechanisms for electron transfer between $[Fe(CN)_6]^{4-}$ and the azurin-covered electrode can be envisaged:[27] (1) the electroactive species could permeate through the protein monolayer and react at the electrode surface; (2) the electroactive species could directly diffuse to bare spots on the electrode through pores or defects of the film; and (3) electrochemical electron transfer could occur via electron exchange with adsorbed azurin. None of the three mechanisms

(27) See for example: Porter, M. D.; Bright, T. B.; Allara, D. L.; Chidsey, C. E. D. *J. Am. Chem. Soc.* **1987**, *109*, 3559−3568.

can, in principle, be ruled out. The first two pathways are apparently consistent with the present experimental observations and properties of the azurin monolayer film. Particularly, unlike alkanethiol SAMs, the protein film is considerably hydrophilic which would facilitate the permeation of $[Fe(CN)_6]^{4-}$. Moreover, the spots *occupied* by sulfur headgroups on the electrode surface are much smaller in number for the azurin monolayer than for small alkanethiol monolayers (about 2:100, estimated from the surface coverage or molecular size difference). This means that many more *bare* spots on the electrode surface are available in the case of azurin. In each of the first two mechanisms the distorted voltammetric peak shape could be caused by hampered electron exchange between $[Fe(CN)_6]^{4-}$ and the Au(111) surface and partial conversion from planar to radial diffusion. For the third mechanism, i.e., electron exchange between $[Fe(CN)_6]^{4-}$ and adsorbed azurin, azurin$(Cu^{2+/+})_{ads}$, the two equilibrium reduction potentials are close enough (~400 and 375 mV, respectively) that electron transfer in both directions is thermodynamically feasible. The electron-transfer processes in homogeneous solution are also known to be fast and within the time range of the voltammetric scans. Electron transfer between $[Fe(CN)_6]^{4-}$ and azurin$(Cu^{2+/+})_{ads}$ would distort the voltammetric shape toward a sigmoidal shape and still be approximately in keeping with the observed rate pattern. The significantly lower cathodic peak height would finally reflect preferential consumption of the oxidized $[Fe(CN)_6]^{3-}$ form, in line with the slightly higher reduction potential of $[Fe(CN)_6]^{3-/4-}$ compared with that of azurin.

Long-Range Interfacial Electron Transfer of Adsorbed Azurin. Direct electron exchange of adsorbed azurin with Au(111) could not be detected from the CV measurements. Specific reasons for this are discussed below. However, differential pulse voltammograms show both a cathodic and an anodic peak at almost identical potentials around 100 mV (Figure 7A, curves b and b′), which is close to the equilibrium potential of azurin. The peaks are stable and reproducible, and no such responses are associated with Zn-azurin (Figure 7B, curves b and b′) and cystine (Figure 7C, curves b and b′). Observations similar to curves b and b′ in Figure 7A are obtained for preadsorbed azurin in contact with azurin-free medium. These results indicate clearly that the peaks are associated with electron exchange between the electrode and the copper center of adsorbed azurin. The Faradaic charge estimated from either

$$\text{azurin}(Cu^{2+})_{ads} + e^- \leftrightarrow \text{azurin}(Cu^{+})_{ads} \qquad (1)$$

cathodic or anodic peaks is about 6.0×10^{-7} C·cm^{-2}, corresponding to about 6.2×10^{-12} mol·cm^{-2} azurin molecules. This agrees with the results based on reductive desorption measurements and suggests that almost all azurin molecules in the monolayer retain their function.

The EIS provides a feasible, if not unique, way to determine the apparent rate constant (k_{et}') of the interfacial ET for the present case. The EIS measurements were conducted under various experimental conditions to be optimized. Suitable frequencies were found to be in the range from 100 Hz to 250 kHz. No detectable difference was observed in the EIS spectra when the electrode potential was set in the range 50−100 mV. Beyond this range, the measured impedance at low frequencies depends strongly on the electrode potential as expected. This is indicative that the surface formal potential of adsorbed azurin is in the range of 50−100 mV and consistent with the DPV observations (Figure 7A). Figure 8 shows a suitable equivalent circuit (A) and measured values with an electrode potential of 100 mV and simulated impedance (B). In the equivalent circuit

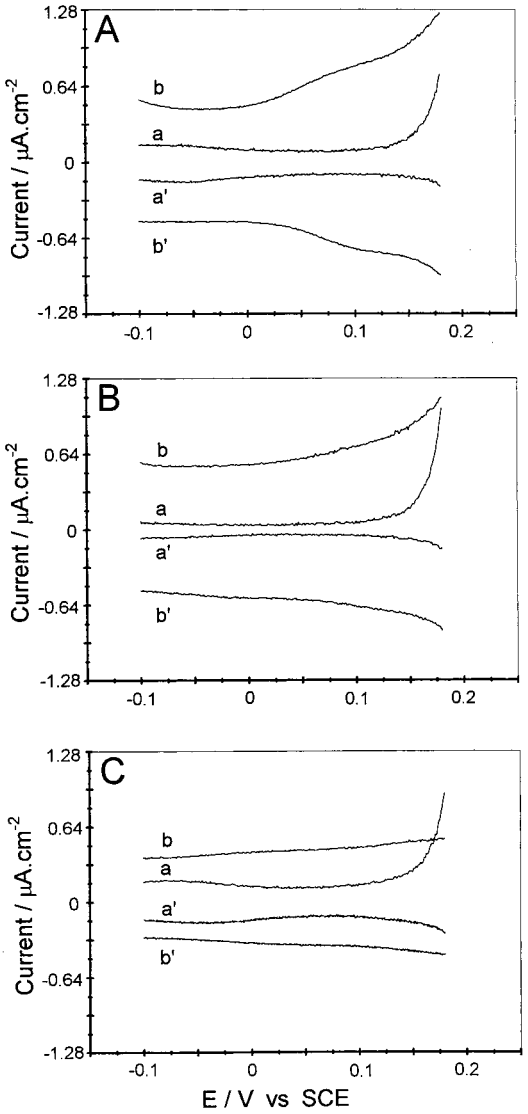

Figure 7. Differential pulse voltammograms of Au(111) in 50 mM NH_4Ac (pH 4.6) containing Cu-azurin (A), Zn-azurin (B), and cystine (C). (A, B) Azurin concentrations (a, a′) 0 and (b, b′) 1.5×10^{-7} M. (C) Cystine concentrations: (a, a′) 0 and (b, b′) 5.0×10^{-6} M. Curves a and b were recorded with potential scans from −0.1 to 0.18 V, curves a′ and b′ from 0.18 to −0.1 V.

shown in Figure 8A, R_s is the solution resistance, C_{dl} represents the double-layer capacitance, R_{ct} is the charge-transfer resistance, C_a is the adsorption pseudocapacitance related to the redox process, and R_a is a resistance reflecting background Faradaic current.[28a] A convenient method to estimate the rate constant uses the following equations:[7c,28]

$$\Gamma = 4RTC_a/n^2F^2A \qquad (2)$$

$$k_{et}' = 2RT/n^2F^2A\Gamma R_{ct} \qquad (3)$$

where Γ is the surface coverage of azurin. Other symbols have been described above or have their usual meaning. A simple equation for estimating k_{et}' is thus

$$k_{et}' = {}^1/_2 R_{ct}C_a \qquad (4)$$

In the present case, the charge-transfer resistance (R_{ct}) is relatively large so that R_a cannot be omitted from the circuit (Figure 8A). The apparent rate constant estimated for ET

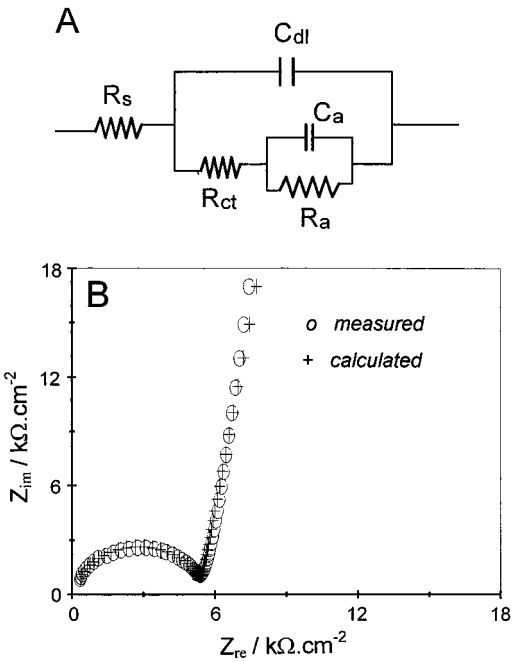

Figure 8. (A) Equivalent circuit used in the simulations and (B) Cole−Cole plots of electrochemical impedance spectra for Cu-azurin-adsorbed Au(111) in 50 mM NH_4Ac (pH 4.6). Marks of "+" and "O" indicate respectively calculated and measured values. The potential was set at the surface formal potential of 0.1 V vs SCE. Amplitude voltage, 5 mV. Frequency range, 100 Hz to 250 kHz.

between adsorbed azurin and Au(111) according to eq 4 is 30 ± 5 s^{-1}. This is lower than that for cytochrome *c* adsorbed directly on a poly-Au electrode (about 130 s^{-1}),[28a] azurin adsorbed on hexanethiol-modified poly-Au electrode (ca. 300 s^{-1}),[29] and azurin immobilized at pyrolytic edge-plane graphite electrodes (up to 5000 s^{-1}).[30] This is due to both the different orientation and the different adsorption modes of the protein molecules. For example, the pattern for azurin adsorption on hexanethiol-modified polycrystalline Au[29] is likely to involve contact with the hydrophobic protein surface area around the copper atom. The fast electron exchange described in ref 30 is likely to be associated with a similar azurin orientation and a significantly shorter electron-transfer distance. In the present case, the adsorption is via the disulfide group. The distance between the copper center of adsorbed azurin and the electrode surface is then about 25 Å, compatible with a long-range ET mode. Long-range ET, from the disulfide anion radical prepared by pulse radiolysis and the copper atom in wild-type and many mutant azurins, has been extensively reported.[8b,9,31] The intramolecular rate constant for wild-type azurin is ∼44 s^{-1}. This is, in fact, a small value compared to the present value as the latter refers to the exchange rate constant close to equilibrium whereas the pulse radiolysis-based data represent a strongly exothermic process. The environmental protein and solvent reorganization Gibbs free energies are, however, also different in the two cases due to the proximity of the metal electrode in the electrochemical case.

The absence of a cyclic voltammetric signal from the copper center of azurin adsorbed via the disulfide group, despite an interfacial ET rate constant of 30 s^{-1}, is apparently unexpected. There could be three reasons for this. First, the surface concentration of adsorbed azurin at Au(111) even for a closed-packed monolayer is lower compared with that of the polycrystalline electrodes used in refs 7c, 28a, 29, and 30. This could result in a weak signal. Second, the voltammetric peaks, as apparent from the DPV data (Figure 7), are broad and indicative of dispersion of the rate constants. The presence of the azurin adlayer induces, finally, a considerable inflation effect as shown in Figures 2 and 3, which could bury the redox signal from adsorbed azurin. In contrast, cytochrome *c*[7c] or azurin[29] adsorbed at alkanethiol-modified Au electrodes does not cause a notable inflation effect in the CV responses, which facilitates observations of the redox signal directly from CV even at a low rate constant (e.g., 0.4 s^{-1}).[7c]

Overall, the results described above enable us to summarize the major molecular events of azurin on Au(111) in Figure 9. The scheme includes adsorption, reductive desorption, and electron transfer across the protein and the interface between the protein and the electrode.

Concluding Remarks

Spontaneous adsorption of protein molecules directly on solid metal electrodes, i.e., in the absence of promoters or other surface pretreatments, is frequently undesirable due to the loss of protein function, i.e., denaturation. The results in the present report show, however, that suitable natural linker groups such as the Cys3Cys26 disulfide group in *P. aeruginosa* azurin can lead the protein to adsorb in a stable functional monolayer on Au(111).

First, the data are comprehensive and include results from cyclic and differential pulse voltammetry, electrochemical impedance spectroscopy, X-ray photoelectron spectroscopy, and electrochemical in situ scanning tunneling microscopy. The voltammetric and impedance spectroscopic data show clearly that azurin adsorbs from NH_4Ac buffer at submicromolar concentrations in a broad electrochemical potential range. The voltammetric data also follow the patterns for the two reference molecules used Zn-azurin and cystine. Reductive desorption at significantly negative potentials is, particularly, a feature, and the charge associated with this two-electron-transfer step accords well with monolayer formation of all three molecules. This feature also characterizes zinc-substituted azurin.

Second, it is presently an open question to which extent the disulfide bond is broken on azurin adsorption. Indications based on high-resolution in situ STM of small organic disulfides show that these images are indistinguishable from images of the corresponding thiolate monomers.[32] There are also indications based on azurin mutants that bond breaking of the disulfide group in azurin strongly destabilizes the protein.[33] In the present case, binding of the two thiolate groups to the Au(111) surface would, however, be expected to assist in retaining a stable three-dimensional structure.

Third, adsorption of the protein in largely integrated form is supported by the following lines of evidence:

(a) Differential pulse voltammetry discloses an azurin signal around the bulk equilibrium reduction potential. This signal is absent for the three reference molecules, i.e., cysteine, cystine, and Zn-azurin, and likely to be associated with oxidation and reduction of the copper center in adsorbed but functional azurin.

(28) (a) Sagara, T.; Niwa, K.; Sone, A.; Hinnen, C.; Niki, K. *Langmuir* **1990**, *6*, 254−262. (b) Nahir, T. M.; Bowden, E. F. *J. Electroanal. Chem.* **1996**, *410*, 9−13.

(29) Gaigalas, A. K.; Niaura, G. *J. Colloid. Interface Sci.* **1997**, *193*, 60−70.

(30) Hirst, S.; Armstrong, F. A. *Anal. Chem.* **1998**, *70*, 5062−5071.

(31) Farver, O.; Skov, L. K.; Van de Kamp, M.; Canters, G. W.; Pecht, I. *Eur. J. Biochem.* **1992**, *210*, 399−403.

(32) Wan, L. J.; Hara, Y.; Noda, H.; Osawa, M. *J. Phys. Chem. B* **1998**, *102*, 5943−5946.

(33) Bonander, N.; Karlsson, B. G.; Vanngard, T. *Biochim. Biophys. Acta* **1995**, *1251*, 48−54.

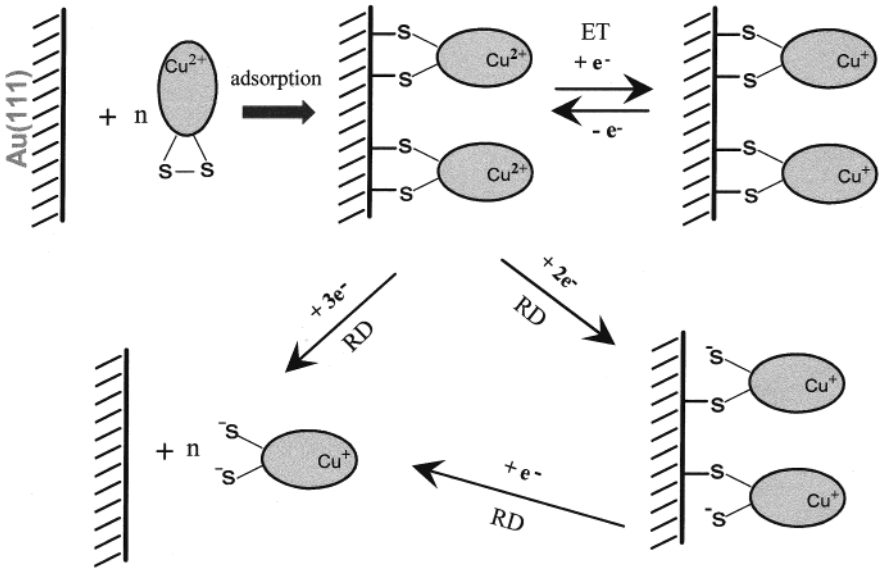

Figure 9. Proposed pattern for adsorption, reductive desorption (RD), and electron transfer (ET) of azurin on Au(111).

(b) Analysis of the electrochemical impedance data gives a value of ca. 30 s^{-1} for the rate constant for interfacial electron transfer between the copper center and the electrode surface. This can be compared with the rate constants for intramolecular electron transfer between the copper center and either the disulfide anion radical (44 s^{-1})[31] or surface-attached $Ru^{3+/2+}$ complexes (10^2-10^6 s^{-1}).[10] Comparison of the rate constants must, however, incorporate the rather different driving forces and environmental reorganization Gibbs free energies. For example, the driving force for the intramolecular electron transfer from the disulfide anion radical to Cu^{2+} is about 700 mV. The driving force of the Ru-modified azurins is also large, and electron transfer is along different tunneling routes through the protein. The driving force for the interfacial process is about zero. This difference would, in fact, give a much larger difference between the rate constants than that observed unless the reorganization Gibbs free energy for the interfacial process is correspondingly smaller than that for the intramolecular process in homogeneous solution.

(c) The XPS data show that adsorption is via sulfur groups, but a spectroscopic feature from the copper ligand sulfur atoms which are not in direct contact with the gold surface can also be distinguished.

(d) In situ STM of adsorbed azurin, finally, shows that a stable dense monolayer where individual molecules can be clearly distinguished directly in the natural aqueous medium is formed persistently.

The comprehensive approach in this work, based on integrated use of electrochemistry, surface spectroscopy, and in situ STM, has provided a quite detailed characterization of an adsorbed monolayer of a functional redox metalloprotein on a metal surface. The methods used are broadly known from studies of self-assembled monolayers of alkanethiols and other sulfur-containing and sulfur-free small molecules. The present investigation shows that the methods can be extended to a protein well suited for gentle linking to a metal surface. The disulfide group of azurin has been crucial in this case. Strategic use of other metalloproteins and metalloprotein mutants can, however, introduce or leave other groups in the metalloprotein surface suitable for linking the protein to metallic surfaces in well-defined orientations. Broader investigations of structure−function relationships of immobilized metalloproteins in different supramolecular architectures on single-crystal electrodes, along the lines in this report and with appropriate theoretical support, are in progress.

Acknowledgment. Financial support from the Danish Research Academy, The Danish Technical Science Research Council, Brødrene Hartmann's, the Carlsberg, Novo Nordisk, Daloon, and P.A. Fisker's Foundations is acknowledged. I.C. acknowledges support from ICAT, DTU. We thank G. Warmerdam for her assistance in the isolation and checking of Zn-substituted azurin samples.

Supporting Information Available: Figures S1 and S2, giving responsive characteristics of voltammetry and capacitance of clean Au(111) in various electrolyte solutions; Figures S3 and S4, giving cyclic voltammograms and potential-dependent capacitance curves upon the addition of azurin with various concentrations; and Figures S5 and S6, giving reductive desorption characteristics of azurin and cystine, respectively, adsorbed on Au(111) (PDF). This material is available free of charge via the Internet at http://pubs.acs.org.

JA993174T